This article has been accepted for publication in a future issue of this journal, but has not been fully edited. Content may change prior to final publication. Citation information: DOI 10.1109/TPWRS.2017.2672569, IEEE Transactions on Power Systems

Power Sharing in Angle Droop Controlled Microgrids

Ramachandra Rao Kolluri*, *Student Member, IEEE,* Iven Mareels, *Fellow, IEEE,* Tansu Alpcan, *Senior Member, IEEE,* Marcus Brazil, Julian de Hoog, *Member, IEEE* and Doreen Anne Thomas, *Senior Member, IEEE*

***Abstract*—Component mismatches and parameters drifts drastically affect stability and long-term operation of droop-controlled inverter-based microgrids. This paper analyses and illustrates the impact of design variations and parameter drifts between angle droop controlled inverter interfaced sources in a microgrid. It is shown that microgrid stability is very sensitive to parameter drifts, especially in frequency. A coordination control scheme that uses inter-node communications is proposed for improving the stability margin and ensuring the desired power sharing. Conditions for stability are derived and simulation results are presented to validate the performance of the proposal.**

***Index Terms*—AC microgrids, active power sharing, autonomous microgrid, distributed control, droop control, microgrids, power system reliability, power system stability, smart grids and synchronization.**

I. Introduction

In recent years, integration of renewable energy and storage has become an increasingly common phenomenon in the electricity industry. With rising atmospheric carbon dioxide levels and a push to promote greener technologies, a major transition into renewable energy seems imminent. These renewable energy sources tend to be distributed throughout the grid. Microgrids, therefore, appear as a natural extension to this decentralization of generation [1].

Conventional inertial generation is well understood and its availability is very important to easily maintain the voltage and frequency levels. Despite the fact that microgrids are envisioned as exciting opportunities, providing all the services identical to the traditional electrical power system is not straightforward. To this end, it is important to be able to implement (islanded) microgrids that provide at least the same levels of reliability, robustness and stability that the traditional grid model provides. In fact, the reliability levels have to be higher than in traditional grids given that the loads can be un-interruptible. To facilitate such a design the distributed energy generation in the microgrid should be able to compensate for the loss of grid i.e., regulate the voltage and frequency within permissible levels and also maintain stability and synchrony in the microgrid. In addition, the amount of energy (power) available for dispatch is a crucial limiting factor for microgrid operation. These limits dictate the stability and power supply boundaries of the system. Robust power sharing capability between sources in a microgrid is more of a necessity than a flexibility in such an energy / power limited scenario.

Power sharing between inverter based sources through droop control was first proposed in [2]. Drawing motivation from the operation of synchronous generators, droop controlled inverters measure their output real and reactive power to modify their frequency and voltage, respectively. Certain design criteria ensure proportional power sharing can be achieved between inverters. Since inverters are operated as voltage sources, the droop control based operation is a master-less control. Over the years, various modifications have been introduced to droop control to broaden the spectrum of its applicability. For example, a transformation method is used in [3] to facilitate droop control at various voltage levels. A review of several control techniques used in power sharing between inverter based sources is given in [4].

One well known decentralized control technique is the angle droop control introduced in [5]. Implemented only on real power (P_i - for highly inductive networks), this scheme is motivated by the well-known fact that small angle differences will cause a change in the power sharing between the sources. Therefore, each inverter i is controlled to change its phase angle (δ_i) according to its real power (P_i) output. Depending on the network characteristics, the angle droop control is also modified to control the real or reactive power flow in microgrid networks [6]. Although their implementation is supposedly harder than frequency droop control, angle droop controlled inverter based systems provide better stability margins [7], [8]. Unlike the frequency droop control [2], angle droop control regulates frequency to its set point without steady state error [5]. Some recent papers [9] proposed techniques that also ensure zero steady state deviation.

Besides frequency regulation, power sharing is essential. In angle-droop controlled inverters power sharing is affected by the network impedances and frequency mismatches as well as implementation issues in the control loops. Most of the research work in inverter interfaced microgrids based on droop

*Corresponding author email: rkolluri@student.unimelb.edu.au. This work has been partly funded by a Linkage Grant supported by the Australian Research Council, Better Place Australia and Senergy Australia. R. R. Kolluri, I. Mareels, T. Alpcan and M. Brazil, are with the Department of Electrical and Electronic Engineering, The University of Melbourne, Australia. D. A. Thomas is with the Department of Mechanical Engineering, The University of Melbourne, Australia. J. De Hoog is with IBM Research – Australia, 19/60 City Road, Melbourne VIC 3006 Australia.

This article has been accepted for publication in a future issue of this journal, but has not been fully edited. Content may change prior to final publication. Citation information: DOI 10.1109/TPWRS.2017.2672569, IEEE Transactions on Power Systems

control focuses on the stability and efficiency of these systems under a variety of assumptions. The authors of [10], [11] consider the significance of computational delays, numerical errors and parameter uncertainties and how these affect the power sharing. In [10] a robust controller was proposed to mitigate the adverse effects. No efforts were made to analyse the effects of implementation errors affecting frequency or phase angle. Some authors do acknowledge that frequency or synchronization errors may arise but do not characterise the consequences of such disturbances on power sharing or frequency stability in the network [10], [12], [13], [4]. While it is understood that frequency (angle) related errors do occur, e.g. as a consequence of crystal inaccuracies, inaccurate pre-synchronization of inverter interconnection [12], most papers assume that frequency is accurately implemented. Some of our earlier papers consider the issues arising from frequency mismatches in frequency droop controlled systems [14] and angle droop controlled systems [15].

A. Contribution

In this paper, we analyse the power sharing properties of angle-droop controlled systems under different network topologies. We identify the limitations of implementation and power sharing correction techniques discussed in the literature [6], [7]. The main contributions of this paper are two fold. Firstly small frequency variations are natural in inverters but are largely ignored in the literature; here it is demonstrated that their mere presence destabilises the desired microgrid power distribution equilibrium. Subsequently, inspired by consensus based frequency restoration [16] and consensus based droop control techniques [17], a new consensus control algorithm is presented to overcome frequency noise in the microgrid, and to improve/restore the desired power distribution equilibrium in the microgrid. We also present results that demonstrate the stability of the proposed control methods.

B. Outline

This paper is organised as follows. Section I gives a brief introduction to power sharing via angle droop control which also serves to motivate the issues under consideration in the remainder of the paper. Section II describes the microgrid network topology considered in this paper. It also presents typical inverter models, valid in the context of power dispatch, to indicate how a desired power distribution equilibrium may be realised in an inverter based microgrid. Section III discusses the fundamentals of angle droop control and in particular discusses the effect various control and system parameters have on the power sharing between inverters. A new control methodology is then proposed in section IV, to overcome impedance distribution effect and local clock errors and retain the stability of the desired power sharing equilibrium. Stability properties are discussed in this same section. Section V illustrates the results using a number of simulations. Final comments including pointers to further work conclude the paper in Section VI.

II. System Set-up

A. Inverter modelling

Based on literature, we consider the traditional inverter model where the switching and the inner control loops are at much higher frequencies than its output frequency [18]. This allows us to denote the inverter as an averaged voltage source which is capable of bidirectional power supply and whose output voltage is given by

$$v_i(t) = V_i \cos(\omega t + \delta_i), \tag{1}$$

where t is the time, V_i is the voltage amplitude, ω is the controllable operating frequency and δ_i is the controllable phase angle. For a local time, t_i as perceived at inverter i the output voltage is denoted as:

$$v_i(t_i) = V_i \cos(\omega t_i + \delta_i). \tag{2}$$

B. Modelling the impact of clock drifts

In this paper, we particularly focus on the consequences of clock accuracy, and the impact this has on implementing a global frequency across the microgrid. The majority of the literature generally assumes that the inverters can maintain a particular nominal frequency, yet this nominal / operating frequency can fluctuate. As there are no synchronous machines, there is a compelling case to considering the consequences of clock drift. In practice, as a consequence of clock drift, an inaccuracy of 0.1% in frequency is quite typical in commercial inverters [19], [20], [21] (see also Table I). In a grid connected scenario, these inaccuracies may lead to some fluctuations in power factor but, in autonomous microgrid operations they have much larger implications. In a critical-load and energy-limited scenario, these small fluctuations will hamper the system performance and may affect the system's lifetime.

To facilitate such an analysis, we denote the voltage at each inverter in terms of a common reference time t and represent the local time t_i at the ith inverter with respect to the reference time t as [22]:

$$t_i = t(1 + \epsilon_i), \tag{3}$$

where ϵ_i is the drift of the local clock with respect to the reference clock. Here we consider a time invariant drift, ϵ_i. The stability results will allow us to infer robustness with respect to slowly time varying drifts. When there is no master clock in the system a drift in local clocks is natural.

From the above definitions the ith inverter based source can be modelled in terms of the reference time t (with a slight abuse of notation) as

$$v_i(t) = V_i \cos(\omega_i t + \delta_i), \tag{4}$$

where V_i the voltage amplitude, $\omega_i = \omega + \eta_i$ with $\eta_i = \epsilon_i \times \omega$ is the frequency generated by inverter i and δ_i is the phase angle.

Using commonly reported values for the clock drift, ϵ_i a frequency drift in the order of 0.03 Hz (for reference frequencies around 50 or 60 Hz) is to be expected, as seen in

This article has been accepted for publication in a future issue of this journal, but has not been fully edited. Content may change prior to final publication. Citation information: DOI 10.1109/TPWRS.2017.2672569, IEEE Transactions on Power Systems

Table I. The table lists $\eta = \epsilon\omega$ as well as the corresponding per unit time scale variable $\gamma = 1/(1+\epsilon)$.

Table I: Drifts in commercial inverters

Reference	$\lvert\eta\rvert$(Hz)	γ
[19]	0.05	1 ± 0.001
[20]	0.025	1 ± 0.0005
[21]	0.05	1 ± 0.001
[23]	0.06	1 ± 0.001
[24]	0.025	1 ± 0.0005

On the assumption that the reference signal $v_{i,ref}(t_i)$ is perfectly tracked by the inner (voltage/current) control loops of the inverter, any changes to the reference signal, either in voltage amplitude and/or frequency are reflected by equivalent proportional changes in the output voltage. For proper voltage reference tracking, the reference signal $v_{i,ref}(t_i)$ at each inverter is assumed to be a constant value within the carrier interval, i.e., the switching frequency [25]. This essentially means that any control that changes the reference signal should not act faster than the switching dynamics.

The integration process at each inverter will be affected by the clock drifts. Using (3), we can express the local integration/differentiation as follows,

$$\frac{d(\cdot)}{dt_i} = \gamma_i \frac{d(\cdot)}{dt}, \tag{5}$$

where $\gamma_i = 1/(1+\epsilon_i)$, is a variable that describes how the local clock deviates from the global clock.

III. Angle Droop and Power sharing

A. Introduction to angle droop

According to classical analysis [26] which assumes that all the voltage sources and loads in Figure 1 are operating at an exact common frequency, for example 50Hz, the voltage sources of the form (4) can be represented by their phasor notation $V_i\angle\delta_i$. If we assume that the network impedances have a high X/R ratio and the voltage amplitudes are constant, we have power flow

$$P_{i0} \approx V_i V_0 \sin(\delta_i - \delta_0)/X_{i0}. \tag{6}$$

Assuming the difference between the phase angles is small, we can write:

$$(\delta_i - \delta_0) \cong \chi_{i0} P_{i0} \tag{7}$$

where $\chi_{ij} \triangleq X_{ij}/(V_i V_j)$, is a constant that determines the reciprocal of maximum real power flow between any two nodes in a network in terms of the voltages and line impedance. As seen in (7), the amount of real power flowing between two nodes can be controlled by manipulating the phase angle at the inverter. This forms the basis of the *proportional* angle droop controller [5]:

$$\delta_i \quad = \delta_i^* - m_i(P_i - P_i^*), \tag{8}$$

where m_i is the droop coefficient and $(\cdot)^*$ represent nominal values.

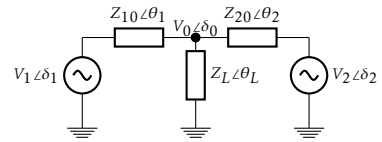

Figure 1: Power flow within a system consisting of two voltage sources supplying a common load.

Observe that the implementation of angle droop control requires a common clock signal and the angle measurements are made with respect to a common angular frequency ω^* (50 or 60 Hz for example) [6]. Using the global positioning system (GPS) based time synchronization was presented as a possible solution for time synchronization in [6]. A disadvantage of such design is that the entire network is dependent on an external timing source, which indicates a single point of failure.

B. Effect of line impedances on power distribution

The main aim of the angle droop controller is to provide robust and fair power sharing without imposing a master-slave relationship on the system. Therefore, it is important to understand how the power sharing between the inverters is achieved using angle droop control.

1) Two source one load case: In this case, the angle differences between the sources and the load of Figure 1 can be given by (7) as follows:

$$(\delta_1 - \delta_0) \cong \chi_{10} P_{10}, \tag{9}$$

$$(\delta_2 - \delta_0) \cong \chi_{20} P_{20}. \tag{10}$$

Assuming that the sources 1 and 2 are operated on angle droop control and also assuming $\delta_i^* = m_i P_i^* = 0$, the angle between the two sources can be represented by (11). Solving equations (9), (10) together with (11) yields (12).

$$(\delta_1 - \delta_2) \cong m_2 P_{20} - m_1 P_{10} \tag{11}$$

$$P_{10}(\chi_{10} + m_1) = P_{20}(m_2 + \chi_{20}) \tag{12}$$

It can be seen from (12) that only a choice of $m_i >> \chi_{i0}$ will result in the desired power sharing ratio $m_1 P_{10} \approx m_2 P_{20}$. If $m_i << \chi_{i0}$ or if there exists a non-negligible link resistance, then we require a more sophisticated technique to ensure proper power sharing.

2) Other topologies: The power sharing correction for topologies like those shown in Figures 2 and 3 is more complex. For the system shown in Figure 2 load voltage communication or central controller based supervision may be used to implement a power sharing correction [6], but such systems are then susceptible to a single point-of-failure. Also this solution is difficult to scale, as any change in the topology require a change in the control law. For the system in Figure 3, choosing δ_i^* or $m_{i,\text{new}}$ to counteract the power sharing error is difficult due to the unavailability of partial power terms. Measuring partial power terms for δ_i^* correction is impractical and even load voltage feedback will not guarantee power sharing. For more discussion along these lines refer to [15].

This article has been accepted for publication in a future issue of this journal, but has not been fully edited. Content may change prior to final publication. Citation information: DOI 10.1109/TPWRS.2017.2672569, IEEE Transactions on Power Systems

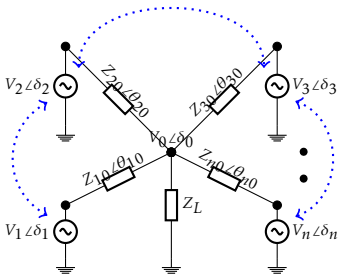

Figure 2: Star topology - n angle droop controlled inverter systems supplying a common load Z_L. Each inverter is represented by a phasor $V_i\angle\delta_i$ and is connected to the load $(V_0\angle\delta_0)$ through an output impedance $Z_{i0}\angle\theta_{i0}$. The blue dotted lines represent communication between inverters as introduced in section IV.

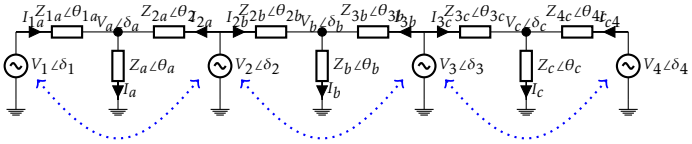

Figure 3: Four inverter three load microgrid. The blue dotted lines represent communication between inverters as introduced in section IV.

To the best of our knowledge, in the literature no control method using only limited communications can adequately ensure fair power sharing in angle droop controlled systems. Selecting large values for m_i or modifying m_i based on load voltage communication may provide power sharing, but (especially when $X_{ij}/(V_i V_j)$ is large) this will erode the stability margin of the microgrid system [6], and hence this is not a practical approach. Also obtaining accurate information on X_{ij} for all branches in a network is difficult.

C. Effect of clock drift on power distribution

Let us consider how the power sharing between inverters is affected by clock drift. First, define the average frequency in the network as

$$\omega_{avg} = \frac{1}{n}\sum_{i=1}^{n}\omega_i. \tag{13}$$

Over a short period of time, the average frequency can be viewed as the global system frequency, and we rewrite the ith inverter local voltage (4) in terms of this average network frequency ω_{avg} as follows,

$$v_i(t) = V_i\cos(\omega_{avg}t + \delta_i'(t)), \tag{14}$$

where $\delta_i'(t) = \delta_i + (\omega_i - \omega_{avg})t$ is a time varying phase angle.

Given any network, we continue our analysis using its Kron reduced form [26]. The active power at the ith inverter, p_i, in the Kron reduced network, using (14), is of the form[1]:

$$p_i = G_{ii}V_i^2 + \sum_{k=1,k\neq i}^{n}|Y_{ik}|V_i V_k\sin(\delta_i' - \delta_k' + \phi_{ik}), \tag{15}$$

where $Y_{ik} = G_{ik} + jB_{ik}$ is the complex admittance and ϕ_{ik} is the admittance angle between inverters i and k in the Kron reduced network. (Recall that the analysis conducted here is with respect to a global reference time t, and a global frequency ω_{avg}.)

The sinusoidal terms in p_i are functions of time due to the clock drifts as follows:

$$\begin{aligned}\sin(\delta_i' - \delta_k' + \phi_{ik}) &= \sin((\delta_i + (\omega_i - \omega_{avg})t) \\ &\quad - (\delta_k + (\omega_k - \omega_{avg})t) + \phi_{ik}) \qquad (16)\\ &= \sin(\delta_i - \delta_k + (\omega_i - \omega_k)t + \phi_{ik}). \qquad (17)\end{aligned}$$

Since in our setting $(\omega_i - \omega_k) = (\epsilon_i - \epsilon_k)\omega$ is not zero, the power flow p_i (15) varies (slowly) with time as a sum of sine functions, each sine function having a small frequency given by the frequency error between two inverters. (Using the data in Table II, observe that the time scale for these power flow variations is in the order of 30 seconds.)

In summary, in order to achieve power sharing, we need a control scheme that can overcome both the line impedance effect and the frequency mismatch effect. To enable such control, and allow the above model over a significant period of time to be valid, we first implement a frequency restoration control to suppress any beating phenomenon caused by frequency differences. We now extend our results from [15] and demonstrate a controller using limited communication that can deliver power sharing in the present scenario.

IV. Modified angle droop and stability analysis

Motivated by the robustness and modularity requirements for a microgrid, we make use of inter-node communications to maintain desired power output and achieve synchronization between inverters.

A. Frequency control

To facilitate frequency synchronization between inverters and to eliminate any frequency beating phenomena, we propose that each inverter i communicates its measured local frequency ω_i to the neighbouring inverters $j \in \mathbf{N}_i$. This type of control is locally executed. Example nearest neighbour communication paths are indicated by blue dotted lines in Figures 2 and 3. The ith inverter then implements an integral action controller to reduce the frequency drift:

$$\gamma_i\dot{\omega}_i = -\psi_i\sum_{j\in\mathbf{N}_i}(\omega_i - \omega_j), \tag{18}$$

where $\psi_i > 0$ is the frequency restoration gain.

B. Power control

In order to facilitate power sharing, we propose that each inverter communicates its output power to all its neighbouring inverters. Inspired by consensus theory [27], we modify

[1]The time argument is neglected for simplicity

This article has been accepted for publication in a future issue of this journal, but has not been fully edited. Content may change prior to final publication. Citation information: DOI 10.1109/TPWRS.2017.2672569, IEEE Transactions on Power Systems

the droop equation (8) by adding an integral action term $z_i(t)$ as shown in (19). The integral action $z_i(t)$ is defined in (20).

$$\delta_i = \delta_i^* - m_i \times (P_i - P_i^*) - z_i, \tag{19}$$

$$\gamma_i \dot{z}_i = k_i \sum_{j \in \mathbf{N}_i} (m_i P_i - m_j P_j)., \tag{20}$$

where k_i is the integral control gain. The integral action serves to enforce power flow sharing, because the equilibrium condition implies power sharing.

C. Convergence and stability analysis

The modified angle droop control system is a combination of two separate controllers, one to achieve frequency convergence and another to achieve consensus in power sharing. We have the following stability results.

Theorem IV.1 (Frequency Consensus). *The frequency controller* (18) *with individual control gains $\psi_i > 0$ achieves frequency consensus irrespective of the remaining system behaviour, provided the communication graph is symmetric and well-connected.*

Proof. First, we rewrite the frequency stabilising controller (18) in vector form as

$$\mathbf{\Gamma}\dot{\mathbf{\Omega}} = -\mathbf{\Psi}\mathbf{L}_c\mathbf{\Omega}, \tag{21}$$

where $\mathbf{\Gamma} = diag(\gamma_i)$, $\mathbf{\Omega} = col(\omega_i)$ and $\mathbf{\Psi} = diag(\psi_i)$, and $\mathbf{L}_c$ is the Laplacian matrix associated with the communication structure. Here the communication structure is symmetric and corresponds to a well-connected communication graph, in which case $\mathbf{L}_c$ is positive semi-definite, with a single zero eigenvalue [27]. A steady state $\mathbf{\Omega}^s \neq 0$ will be reached exponentially because the state transition matrix $-\mathbf{\Gamma}^{-1}\mathbf{\Psi}\mathbf{L}_c$ is negative semi-definite, with a single zero eigenvalue.

The steady state is proportional to the zero-eigenvector of the Laplacian:

$$0_n = -\mathbf{L}_c\mathbf{\Omega}^s \iff \mathbf{\Omega}^s = \alpha 1_n \iff \omega_i^s = \omega_j^s = \omega_{avg}, \tag{22}$$

where 0_n is an n-dimensional vector of all zeros and 1_n is an n-dimensional vector of all 1s. It follows that consensus is reached exponentially fast. □

Remark IV.2. *Because $\mathbf{L}_c$ is symmetric with 1_n as eigenvector associated with its unique zero eigenvalue, it is easily seen that $\sum_i \frac{\gamma_i}{\psi_i}\omega_i(t)$ is independent of time. Hence the final averaged frequency, and the consensus of all frequencies, is therefore given by*

$$\omega_{avg} = \lim_{t\to\infty} \omega_i = \frac{\sum_i \frac{\gamma_i}{\psi_i}\omega_i(t)}{\sum_i \frac{\gamma_i}{\psi_i}}, \ t \geq 0. \tag{23}$$

It is thus equal to the weighted sum of the original frequencies, weighted according to the ratio of clock drift to the corresponding frequency controller gain.

Given all γ_i are near 1, selecting all $\psi_i = \psi > 0$ is a reasonable choice, which yields

$$\omega_{avg} = \lim_{t\to\infty} \omega_i(t) \approx \frac{1}{n}\sum_i \omega_i(t) \tag{24}$$

The accuracy of the frequency consensus algorithm depends on the measurement accuracy of the local frequency. Perfectly accurate local frequency measurements will lead to perfect synchronization (18). In the presence of clock drift some frequency measurement error cannot be avoided, and the above control law will lead to *almost* frequency stabilisation, with a residual error of the order of the mean measurement error over the network (the larger the network the smaller the residual error). Also, the modified angle droop control, to be proposed in Section IV-B is robust with respect to small inaccuracies in frequency measurement, and hence perfect frequency stabilisation is not required.

Although the power sharing is perturbed by the frequency consensus control action, once frequency consensus is reached, the steady state power distribution (15) only depends on the line impedances. As the frequency consensus is guaranteed independent of the power sharing, the power sharing controller can focus on power sharing as if frequency consensus holds.

To model the dynamics of the power controller, assume that the power measurements are obtained as the output of a unity gain, low pass filter, represented by:

$$\gamma_i \dot{P}_i = -f_{p,i}P_i + f_{p,i}p_i, \tag{25}$$

where $f_{p,i}$ is the low pass filter cut-off frequency and p_i is the power supplied by (see equation (15)) the ith inverter.

Definition IV.3. *Define state vectors $\boldsymbol{\delta} = col(\delta_i)$, $\mathbf{P}_m = col(P_i)$, $\mathbf{P}_a = col(p_i)$ and $\mathbf{Z} = col(z_i)$. Define system matrices $\mathbf{\Gamma} = diag(\gamma_i)$, $\mathbf{M} = diag(m_i)$ and $\mathbf{I}_n = diag(1)$. Introduce the power-angle Jacobian $\mathbf{L}_n = \frac{\partial \mathbf{P}_a}{\partial \boldsymbol{\delta}}|_{\delta^s}$. As above, the matrix $\mathbf{L}_c$ is the symmetric, positive semi-definite Laplacian matrix associated with the communication graph [27].*

We also introduce a deviation vector associated with every state vector. For example, $\bar{\boldsymbol{\delta}}$ is the deviation vector for the local phase angle vector $\boldsymbol{\delta}$, defined as:

$$\bar{\boldsymbol{\delta}} = \boldsymbol{\delta} - \boldsymbol{\delta}^s, \tag{26}$$

where $\boldsymbol{\delta}^s$ is the equilibrium vector of phase angles. Similarly deviation vectors are defined for the state vectors ($\bar{\mathbf{P}}_m, \bar{\mathbf{Z}}$) and equilibrium vectors ($\mathbf{P}_m^s, \mathbf{Z}^s$).

Using equations (19), (20), (25) and (26) we can obtain the deviation vector dynamics of the closed loop system. The linearized system is given below:

$$(\mathbf{I}_2 \otimes \mathbf{\Gamma}) \begin{bmatrix} \dot{\bar{\mathbf{P}}}_m \\ \dot{\bar{\mathbf{Z}}} \end{bmatrix} = \underbrace{\begin{bmatrix} -f(\mathbf{I}_n + \mathbf{L}_n\mathbf{M}) & -f\mathbf{L}_n \\ k\mathbf{L}_c\mathbf{M} & 0_{n\times n} \end{bmatrix}}_{:=\mathbf{A}} \begin{bmatrix} \bar{\mathbf{P}}_m \\ \bar{\mathbf{Z}} \end{bmatrix} \tag{27}$$

For simplicity sake, we assumed $f_{p,i} = f$, and $k_i = k$ to be the measurement filter cut-off and the integral control gain at all inverters, respectively. For properties of matrices $\mathbf{L}_n$ and $\mathbf{L}_c$ see [28] and [29], respectively. The eigenvalues of $\mathbf{A}$ defined

This article has been accepted for publication in a future issue of this journal, but has not been fully edited. Content may change prior to final publication. Citation information: DOI 10.1109/TPWRS.2017.2672569, IEEE Transactions on Power Systems

in (27) are the roots of the equation

$$\det(\lambda_{\mathbf{A}}\mathbf{I}_{2n} - \mathbf{A}) = \det(Q(\lambda_{\mathbf{A}})) \tag{28}$$

where $Q(\lambda_{\mathbf{A}}) = \lambda_{\mathbf{A}}^2\mathbf{I}_n + f\lambda_{\mathbf{A}}(\mathbf{I}_n+\mathbf{L}_n\mathbf{M}) + fk\mathbf{L}_n\mathbf{L}_c\mathbf{M}$.

Lemma IV.4. *Given the properties of the matrices $\mathbf{L}_n, \mathbf{L}_c$ and $\mathbf{M}$, the matrix product $\mathbf{L}_n\mathbf{L}_c\mathbf{M}$ has a zero eigenvalue and all the remaining eigenvalues have positive real parts. The real parts of the eigenvalues of $\mathbf{I}_n + \mathbf{L}_n\mathbf{M}$ are always positive.*

Proof: The droop coefficient matrix $\mathbf{M}$ is diagonal with strictly positive entries, and hence it is strictly positive definite. The network laplacian $\mathbf{L}_n$ is associated with a strongly connected graph (of the Kron-reduced network) and therefore its non-zero eigenvalues have a strictly positive real part (there exists a zero eigenvalue of geometric multiplicity one) [28]. We also assume that any vector $v \in \mathbb{C}^n$ and $\mathbf{L}_c\mathbf{M}v(\neq 0_n)$ is not in the null space of $\mathbf{L}_n$ which is reasonable since the matrix $\mathbf{L}_c$ cannot map to its own kernel space, i.e., 1_n. The second part of the claim comes from the fact that the zero eigenvalue of $\mathbf{L}_n\mathbf{M}$ disappears on addition with the identity matrix $\mathbf{I}_n$. □

Theorem IV.5 (Power Sharing). *Considering that the frequency controller (21) stabilizes the frequency, let $\mu_i(= a_i+jb_i)$ be the ith eigenvalue of the matrix $(\mathbf{I}_n+\mathbf{L}_n\mathbf{M})$ and $\rho_i(= x_i+jy_i)$ be the ith eigenvalue of matrix $(\mathbf{L}_n\mathbf{L}_c\mathbf{M})$, $i = 1, 2, \ldots, n$. We define $\sigma := \frac{k}{f}$, $U_i := a_i^2 - b_i^2 - 4\sigma x_i$, and $W_i := 2a_ib_i - 4\sigma y_i$. Then, the linearized closed loop system (27) is stable for appropriate choices of $f, 0 < k << \min(\frac{1}{m_i})$, $0 < m_i << 1$ that satisfy the condition:*

$$\frac{W_i^2}{4} + U_i < 1 \tag{29}$$

Proof. First, we prove that power sharing criterion is satisfied. The integral consensus term of (20) is a negative feedback term with the matrix $\mathbf{L}_c$ governing its state evolution. Consequently, in steady state, we have:

$$0_n = k\mathbf{L}_c\mathbf{M}\mathbf{P}_m^s \iff \mathbf{M}\mathbf{P}_m^s = \beta 1_n \iff m_iP_i^s = m_jP_j^s, \tag{30}$$

where 0_n is a n-dimensional vector of zeros, 1_n is a n-dimensional vector of ones and β is a constant depending on aggregate inverter loading which includes both loads and losses. Secondly, to prove the system stability, we analyse the characteristic polynomial $\det(Q(\lambda_{\mathbf{A}}))$ defined in (28). Recall that from Lemma IV.4, the $\mathfrak{Re}\{v^*\mathbf{L}_n\mathbf{L}_c\mathbf{M}v\} \geq 0$ and $\mathfrak{Re}\{v^*(\mathbf{I}_n + \mathbf{L}_n\mathbf{M})v\} > 0$ for any vector $v \in \mathbb{C}^n$ with $v^*v = 1$. For any vector v with $v^*v = 1$ we will then have

$$v^*Q(\lambda_{\mathbf{A}})v = \lambda_{\mathbf{A}}^2 + f\lambda_{\mathbf{A}}v^*(\mathbf{I}_n + \mathbf{L}_n\mathbf{M})v + fkv^*\mathbf{L}_n\mathbf{L}_c\mathbf{M}v. \tag{31}$$

Let v_i be the right eigenvector of $Q(\lambda_{\mathbf{A}})$, such that $v_i^*Q(\lambda_{\mathbf{A}})v_i = 0$. That implies

$$\lambda_{\mathbf{A}}^2 + f\lambda_{\mathbf{A}}v_i^*(\mathbf{I}_n + \mathbf{L}_n\mathbf{M})v_i + fkv_i^*\mathbf{L}_n\mathbf{L}_c\mathbf{M}v_i = 0. \tag{32}$$

With eigenvalue definitions introduced in the statement of Theorem (IV.5) the above equation becomes

$$\lambda_{\mathbf{A},i}^2 + f\lambda_{\mathbf{A},i}\mu_i + fk\rho_i = 0. \tag{33}$$

The eigenvalues of $\mathbf{A}$ are the roots of the above equation for $i = 1, 2, \ldots, n$. From Lemma IV.4 we conclude that $\mu_1 = 1$ and $\rho_1 = 0$ are the smallest eigenvalues associated with the second and the last term in (32), respectively. Moreover, $\varpi\mathbf{M}^{-1}1_n, \varpi \in \mathbb{R} \setminus \{0\}$ is the eigenvector associated with these eigenvalues. Therefore, we conclude that the first two eigenvalues of the matrix $\mathbf{A}$ are

$$\lambda_{\mathbf{A},1_{1,2}} = 0, -f. \tag{34}$$

The remaining eigenvalues are obtained by solving

$$\lambda_{\mathbf{A},i}^2 + f\lambda_{\mathbf{A},i}\mu_i + fk\rho_i = 0, \quad i = 2, 3, \ldots, n \tag{35}$$

Since the above equation is quadratic, the solutions can be written as

$$\lambda_{\mathbf{A},i} = \frac{f}{2}\left[-1 \pm \sqrt{\mu_i^2 - \frac{4k\rho_i}{f}}\right]. \tag{36}$$

As introduced in the Theorem IV.5 statement, we can define

$$\sqrt{U_i + jW_i} = \sqrt{\mu_i^2 - \frac{4k\rho_i}{f}} \tag{37}$$

The roots of $\sqrt{U_i + jW_i}$ take the form $\pm(u_i + jw_i)$ [28]. Here, we need u_i to be less than 1 to ensure that the (non-zero) roots always have a negative real part, which can be achieved by designing an integral control gain k according to (29). The sign of the eigenvalues of $\mathbf{A}$ will not be affected by the positive-definite matrix $(\mathbf{I}_2 \otimes \mathbf{\Gamma})$. Since traditional angle droop controller is based on small angle approximations (truncated Taylor series expansion) of the sine function, it is good practice to choose small values of k, typically much lesser than the smallest reciprocal of any droop coefficient, i.e., $k << \min(\frac{1}{m_i})$ to avoid unnecessary oscillations. □

V. Simulations and Discussion

We present a simulation example to illustrate the performance of the stabilizing controller; a microgrid consisting of three single phase inverters (controlled using cascaded voltage control loops [30]) operating in parallel supplying a common load, a system in a star topology as discussed in Section III. The parameters of the system are given in Table II. They are informed by [11], [30] and are modified to suit our model. It is worth observing here that the main network impedances are inductive. If these impedances were not inductive, the suggested angle droop controller would be inappropriate. We remark that when this is not the case, virtual impedance control at the inverter can be used to enforce this condition. The simulations are implemented in MATLAB SimPowerSystems. Several scenarios with different controllers are simulated.

Table II: Simulation Parameters

V_{dc}	f_{sw}	k_{pi}	k_{pv}	k_{ri}	k_{rv}	L_f	C_f
380V	10kHz	0.7	0.35	100	400	1.8mH	25μF
V_i	R_1	R_2	R_3	X_1	X_2	X_3	R_0
339.4V	0.02Ω	0.04Ω	0.03Ω	j0.2Ω	j0.4Ω	j0.3Ω	16.6Ω

m_i	ω^*	δ_i^*	$\mathbf{L}_c$
(1×10^{-6})°/W	50 Hz	0°	[1 −1 0; −1 2 −1; 0 −1 1]

This article has been accepted for publication in a future issue of this journal, but has not been fully edited. Content may change prior to final publication. Citation information: DOI 10.1109/TPWRS.2017.2672569, IEEE Transactions on Power Systems

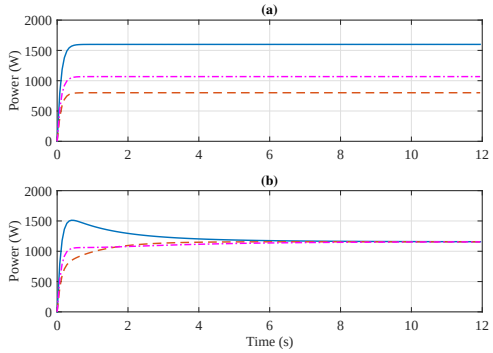

Figure 4: Active power sharing between inverters in (a) traditional angle droop (b) proposed angle droop control with inverters operating at ideal frequencies; – Inverter 1, - - Inverter 2, -.- Inverter 3.

Case 1 : Inverters with identical clocks and disproportionate output impedances

The three inverters are operating at the rated frequency $\omega = 50$ Hz. There are no clock drifts: $\gamma_i = 1$. The evolution of the output power supplied by the inverters in this scenario is given by Figure 4(a). It can be clearly seen that the power supplied by each inverter depends on its output impedance as discussed in section IV. As is to be expected, the inverter with the largest per-unit output impedance supplies the least power.

Case 2 : Inverters with identical clocks, disproportionate output impedances and power consensus controls

In this case, the rated frequency, ω^* at each inverter remains at 50 Hz. Clock drifts are not present. Only the proposed power consensus controllers are now active. Figure 4(b) shows changes in the active power output of each inverter over a time period of 12 seconds. The power consensus time constant is about 1s. It is clearly seen that power sharing is restored. The integral controller ensures zero power sharing error in this case, irrespective of the disparate per-unit output impedances.

Case 3: Inverters with non-identical clocks and disproportionate output impedances

In this case, the rated frequencies of the inverters remain at 50 Hz. Time invariant clock drifts are present. The relevant drift parameters are $\eta_1 = -0.01$ Hz, $\gamma_1 = 1.0002$, $\eta_2 = 0.01$ Hz, $\gamma_2 = 0.9998$ and $\eta_3 = 0.02$ Hz, $\gamma_3 = 0.9996$.

The output power and the local frequency of each inverter is shown in 5(a) and 5(c), respectively. When these clock drift are not compensated for, the injected powers start drifting apart. That is the microgrid is unstable. Indeed notice that in this case one of the inverters actually sink power. Four quadrant inverters may be able to cope with this situation under some energy constraints, but simple inverters will not allow such large deviations, and their current protection will lead to inverter shut-down, and hence microgrid failure. Moreover, as shown in Figure 5(e), the voltage stability of the microgrid has also been compromised. Clearly, there is no stable network frequency (shown in figure 5(g)) in the microgrid.

Case 4: Inverters with non-identical clocks, disproportionate output impedances and consensus controls

While the parameters are the same as in the previous case, in this scenario both the frequency and power consensus controls are active and chosen according to the criteria provided. In spite of the clock drift, it is clearly shown in Figure 5(b) that power sharing is achieved. During the transient phase, the power sharing error is still significant; further work is required to avoid large transient deviations in power sharing, and to respect the operational envelope of the inverters. Once the frequency consensus control delivers a consensus frequency, as shown in Figure 5(d) the power sharing is quickly restored (the time constant was chosen rather large to illustrate the effect of the frequency consensus control). We also observed that the power sharing controller alone can counteract small frequency differences in terms of stability of output power.

In most cases, the large fluctuations in power can be avoided by making proper choices of the control gains k and ψ. For the given system, the large negative power outputs can be avoided by little larger gains. This result is shown in Figure 6. In Figure 6(a) the control gain k is increased to 10^4 which results in smaller fluctuations in the real power output. In Figure 6(b) the frequency control gain is increased to $\psi = 2$ and the power control gain gain $k = 5 \times 10^3$. As shown, the power fluctuations are similar to the case with $k = 10^4$ (with a small negative output). The power sharing error also subsides quickly in both these cases. Since we have assumed that the inverters are bidirectional, they can easily cope with small negative power variations, if any. Desired transient response can be achieved by carefully tuning the control gains. Very large gain k might result in an oscillatory response since the eigenvalues can reach the imaginary axis. This should be avoided to achieve asymptotic stability as remarked at the end of the proof of Theorem IV.5.

Remark V.1. *It is worth mentioning that typical low voltage microgrids, like the one shown in simulations, are confined to relatively small neighbourhoods and the output impedances would most likely be resistive more than inductive. However, it is possible to modify the output impedance to be inductive by taking advantage of virtual impedance emulation techniques [31]. Indeed, one can modify the reference voltage as:*

$$v_{i,ref}^{new}(t_i) = v_{i,ref}(t_i) - i_o(t_i)R_v - L_v \frac{di_o}{dt_i}, \tag{38}$$

where i_o is the output current, R_v and L_v are the desired output virtual resistance and inductance, respectively. Virtual impedance emulation can also be used to achieve proper power decoupling at various voltage levels and impedance ratios. The analysis should therefore consider these values in Kron reduction and power flow.

This article has been accepted for publication in a future issue of this journal, but has not been fully edited. Content may change prior to final publication. Citation information: DOI 10.1109/TPWRS.2017.2672569, IEEE Transactions on Power Systems

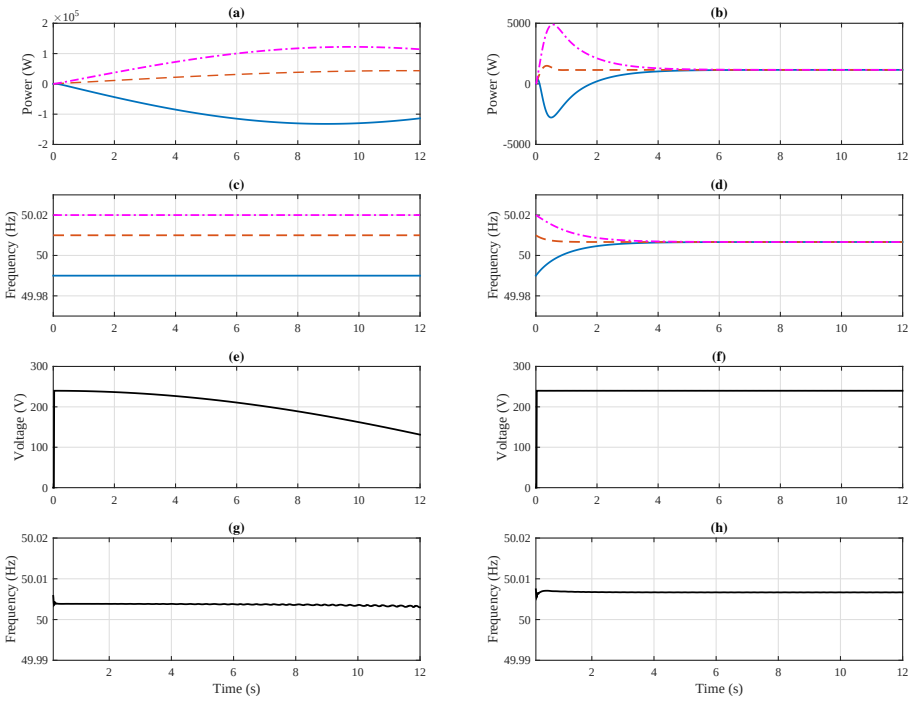

Figure 5: (left) The response of the network with frequency drifts and without consensus control; (right) The response of the network with frequency drifts and with proposed consensus control, $\psi_i = \psi = 1$ and $k_i = k = 10^3$. (a,b) Inverter output active power (c,d) inverter output voltage frequency (e,f) rms load voltage (g,h) load frequency; '–' Inverter 1, '- - ' Inverter 2, '-.-' Inverter 3, '–' Load.

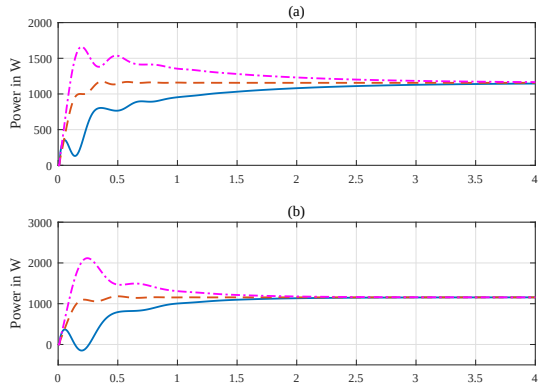

Figure 6: Active power sharing between inverters with (a) $k = 10^4$ and $\psi = 1$ (b) $k = 5 \times 10^3$ and $\psi = 2$; – Inverter 1, - - Inverter 2, -.- Inverter 3.

VI. Conclusion

We have shown that the angle droop controller is very sensitive to clock drift. Assuming the frequency drifts are slowly time varying, we introduced a combination of stabilizing controllers that ensure the desired operation in an angle droop controlled microgrid. The proposed framework is based on local peer-to-peer communication to achieve first a consensus in the system frequency and then to restore the desired power sharing between the inverters. Simulation results are presented to illustrate the control ideas. Transient stability, and safety of grid connected operation of angle droop controlled microgrids as well as communication latency are some important aspects that require further work. A laboratory scale implementation of the proposed microgrid control will be reported separately.

References

[1] R. Lasseter, "Microgrids," in *Power Engineering Society Winter Meeting, 2002. IEEE*, vol. 1, 2002, pp. 305–308 vol.1.

[2] M. Chandorkar, D. Divan, and R. Adapa, "Control of parallel connected inverters in standalone ac supply systems," *Industry Applications, IEEE Transactions on*, vol. 29, no. 1, pp. 136–143, Jan 1993.

[3] K. De Brabandere, B. Bolsens, J. Van den Keybus, A. Woyte, J. Driesen, and R. Belmans, "A voltage and frequency droop control method for parallel inverters," *Power Electronics, IEEE Transactions on*, vol. 22, no. 4, pp. 1107–1115, July 2007.

[4] H. Han, X. Hou, J. Yang, J. Wu, M. Su, and J. M. Guerrero, "Review of power sharing control strategies for islanding operation of ac microgrids," *IEEE Transactions on Smart Grid*, vol. 7, no. 1, pp. 200–215, Jan 2016.

[5] R. Majumder, A. Ghosh, G. Ledwich, and F. Zare, "Angle droop versus frequency droop in a voltage source converter based autonomous microgrid," in *Power Energy Society General Meeting, 2009. PES '09. IEEE*, July 2009, pp. 1–8.

[6] R. Majumder, G. Ledwich, A. Ghosh, S. Chakrabarti, and F. Zare, "Droop control of converter-interfaced microsources in rural distributed generation," *Power Delivery, IEEE Transactions on*, vol. 25, no. 4, pp. 2768–2778, Oct 2010.

[7] R. Majumder, B. Chaudhuri, A. Ghosh, R. Majumder, G. Ledwich, and F. Zare, "Improvement of stability and load sharing in an autonomous microgrid using supplementary droop control loop," *Power Systems, IEEE Transactions on*, vol. 25, no. 2, pp. 796–808, May 2010.

[8] J. Schiffer, A. Anta, T. D. Trung, J. Raisch, and T. Sezi, "On power sharing and stability in autonomous inverter-based microgrids," in *IEEE 51st Annual Conference on Decision and Control (CDC)*, dec. 2012, pp. 1105 –1110.

[9] M. Yazdanian and A. Mehrizi-Sani, "Washout filter-based power sharing," *IEEE Transactions on Smart Grid*, vol. 7, no. 2, pp. 967–968, March 2016.

[10] Q.-C. Zhong, "Robust droop controller for accurate proportional load sharing among inverters operated in parallel," *Industrial Electronics, IEEE Transactions on*, vol. 60, no. 4, pp. 1281–1290, April 2013.

[11] B. Shoeiby, D. Holmes, B. McGrath, and R. Davoodnezhad, "Dynamics of droop-controlled microgrids with unequal droop response times," in *Power Engineering Conference (AUPEC), 2013 Australasian Universities*, Sept 2013, pp. 1–6.

[12] T. Vandoorn, B. Renders, B. Meersman, L. Degroote, and L. Vandevelde, "Reactive power sharing in an islanded microgrid," in *Universities Power Engineering Conference (UPEC), 2010 45th International*, Aug 2010, pp. 1–6.

[13] W. Yao, M. Chen, J. Matas, J. Guerrero, and Z. ming Qian, "Design and analysis of the droop control method for parallel inverters considering the impact of the complex impedance on the power sharing," *Industrial Electronics, IEEE Transactions on*, vol. 58, no. 2, pp. 576–588, Feb 2011.

[14] R. R. Kolluri, T. Alpcan, I. Mareels, M. Brazil, J. de Hoog, and D. Thomas, "On the effect of component mismatches in inverter interfaced microgrids," in *Proceedings of the Australasian University Power Engineering Conference (AUPEC)*, September 2014.

[15] R. R. Kolluri, I. Mareels, T. Alpcan, M. Brazil, J. de Hoog, and D. Thomas, "Power sharing correction in angle droop controlled inverter interfaced microgrids," in *Power Energy Society General Meeting, 2015 IEEE*, July 2015, pp. 1–5.

[16] J. W. Simpson-Porco, F. Dörfler, and F. Bullo, "Synchronization and power sharing for droop-controlled inverters in islanded microgrids," *Automatica*, vol. 49, no. 9, pp. 2603 – 2611, 2013.

[17] L.-Y. Lu and C.-C. Chu, "Robust consensus-based droop control for multiple power converters in isolated micro-grids," in *Circuits and Systems (ISCAS), 2014 IEEE International Symposium on*, June 2014, pp. 1820–1823.

[18] G. Weiss, Q.-C. Zhong, T. Green, and J. Liang, "H infin; repetitive control of dc-ac converters in microgrids," *Power Electronics, IEEE Transactions on*, vol. 19, no. 1, pp. 219–230, Jan 2004.

[19] Schneider Electric, "Conext XW inverter/charger product manual," 2014, [Online; accessed 8-November-2014]. [Online]. Available: http://www.schneider-electric.com/products/au

[20] Emmerson Network Power, "Chloride CP-70i 01 DC/AC inverter datasheet," http://www.emersonnetworkpower.com/documentation/en-us/products/industrialpower/documents/cp-70i/chloride%20cp-70i%2001%20dc-ac%20inverter_dsuk_rev3-062013.pdf, 2014, [Online; last accessed 14-June-2016].

[21] Magnum Dimensions, "The MSH-RE Series Inverter / Charger," http://www.magnum-dimensions.com/sites/default/files/manuals/spec/MSH-RE_series_datasheet_revB_%2364-0498_web.pdf, 2014, [Online; last accessed 14-June-2016].

[22] J. Schiffer, R. Ortega, C. A. Hans, and J. Raisch, "Droop-controlled inverter-based microgrids are robust to clock drifts," in *American Control Conference (ACC)*, June 2015, pp. 2341–2346.

[23] Power Stream, "Rugged, heavy duty and industrial grade 3-phase pure sine wave DC/AC inverters," http://www.powerstream.com/inverter-3-phase-24vdc-208vac-6000w.htm, 2016, [Online; last accessed 14-June-2016].

[24] Yueqing Sandi Electric Co., Ltd, "Solar Sine Wave Inverter," https://www.evworks.com.au/assets/files/Manual%20of%20SDP-10KW%20inverter.pdf, [Online; last accessed 14-June-2016].

[25] D. Holmes and T. Lipo, *Pulse Width Modulation for Power Converters: Principles and Practice*, ser. IEEE Press Series on Power Engineering. John Wiley & Sons, 2003. [Online]. Available: http://books.google.com.au/books?id=8LGi1AjSfpcC

[26] P. Kundur, N. Balu, and M. Lauby, *Power system stability and control*, ser. EPRI power system engineering series. McGraw-Hill, 1994.

[27] R. Olfati-Saber, J. Fax, and R. Murray, "Consensus and cooperation in networked multi-agent systems," *Proceedings of the IEEE*, vol. 95, no. 1, pp. 215–233, Jan 2007.

[28] J. Schiffer, D. Goldin, J. Raisch, and T. Sezi, "Synchronization of droop-controlled microgrids with distributed rotational and electronic generation," in *IEEE 52nd Annual Conference on Decision and Control (CDC)*, Dec. 2013, pp. 2334–2339.

[29] J. Schiffer., T. Seel, J. Raisch, and T. Sezi, "A consensus-based distributed voltage control for reactive power sharing in microgrids," in *13th European Control Conference (ECC)*, June 2014, pp. 1299–1305.

[30] J. C. Vasquez, J. M. Guerrero, M. Savaghebi, J. Eloy-Garcia, and R. Teodorescu, "Modeling, analysis, and design of stationary-reference-frame droop-controlled parallel three-phase voltage source inverters," *IEEE Transactions on Industrial Electronics*, vol. 60, no. 4, pp. 1271–1280, April 2013.

[31] Y. W. Li and C.-N. Kao, "An accurate power control strategy for power-electronics-interfaced distributed generation units operating in a low-voltage multibus microgrid," *Power Electronics, IEEE Transactions on*, vol. 24, no. 12, pp. 2977–2988, Dec 2009.

Ramachandra Rao Kolluri has been a Ph.D. student in Electrical and Electronic Engineering at The University of Melbourne since 2013. His research interests include renewable energy integration in microgrids.

Iven Mareels is Professor of Electrical and Electronic Engineering, and Dean of the Melbourne School of Engineering at The University of Melbourne since 2008. He is an expert in the area of systems engineering.

Tansu Alpcan has been with The University of Melbourne, Australia, since October 2011 where he is currently an Associate Professor. His main research interests are distributed decision making, game theory, and control with applications to energy markets, smart grid, and demand response.

Marcus Brazil is an Associate Professor and Reader in the Department of Electrical and Electronic Engineering at The University of Melbourne. Currently, his main research interests are in Optimal Network Design with a variety of applications.

Julian de Hoog is a Research Staff Member at IBM Research – Australia, and is an Honorary Research Fellow at the University of Melbourne. His research focusses on technical impacts and control strategies for electric vehicles, and integration of renewable generation and storage.

Doreen Thomas is a Professor and Head of the Department of Mechanical Engineering at The University of Melbourne. Her research interests are in network optimisation to applications in a range of areas including power networks and sensor networks.